ORIGINAL ARTICLE

lajss.org
Latin American Journal of Solids and Structures

www.lajss.org

Machine Learning-Based Prediction of Axial Load Bearing Capacity for CFRST Columns

Tuo Lei[a], Jianxiang Xu[a]*, Shuangfei Liang[a], Zhimin Wu[a]

[a]School of Civil Engineering, Chang'an University, Xi'an, 710061. E-mails: leituo616@163.com, 18899530211@163.com, 15532179916@163.com, wuzhimin0903@163.com

*Corresponding author

https://doi.org/10.1590/1679-78257807

Abstract

As a primary load-bearing component, accurately predicting the bearing capacity of concrete-filled rectangular steel tube (CFRST) members is an essential prerequisite for ensuring structural safety. Machine learning methods are employed to model and predict the axial load bearing capacity of CFRST columns. A test database containing 1119 members is established, and the input parameters of the machine learning model are determined using a combination of data preprocessing and correlation analysis. Four machine learning algorithms, namely Lasso, ANN, RF, and XGBoost, are selected to build the prediction models for axial load bearing capacity, and a comparative analysis of their predictive performance is conducted. The feature importance analysis is performed using the SHAP method. The results indicate that the model based on the XGBoost algorithm achieves the highest prediction accuracy. Through comparison with six existing calculation methods in domestic and international codes, the reliability of its predictive performance is verified.

Keywords

Rectangular concrete filled steel tube, Axial compression, Machine learning, Correlation analysis, Bearing Capacity Prediction.

Graphical Abstract

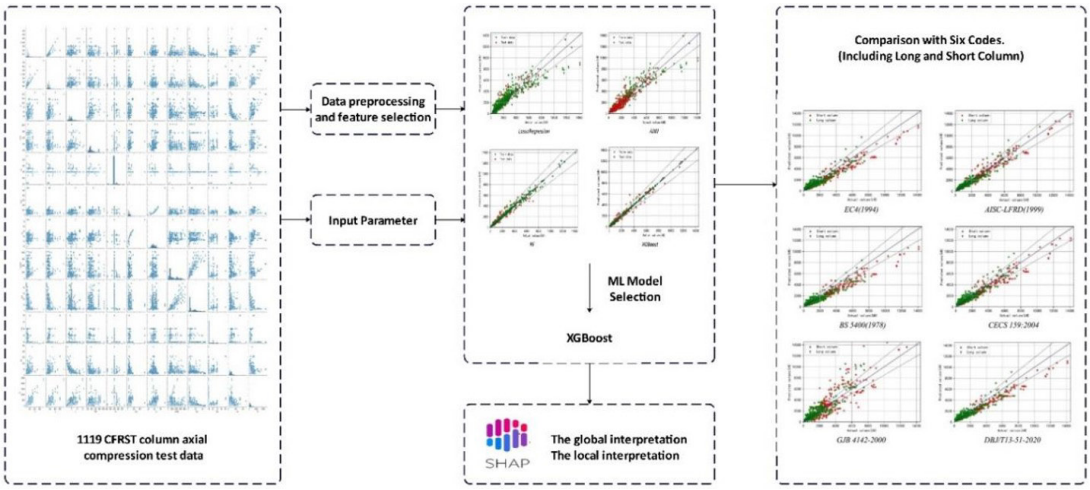

Received: August 22, 2023. In revised form: August 25, 2023. Accepted: September 03, 2023. Available online: September 14, 2023.
https://doi.org/10.1590/1679-78257807

1 INTRODUCTION

Since its inception in the 1940s, artificial intelligence (AI) has been applied in various disciplines and has given rise to multiple algorithms. Machine learning, a major subfield of AI, focuses on the design and development of algorithms that can identify complex patterns from experimental data, without assuming pre-established equations as models, and make intelligent decisions. In comparison to conventional numerical simulation methods, machine learning methods rely on the patterns observed in a large volume of experimental data, with relatively less influence from the user. Moreover, machine learning can effectively utilize existing experimental data, thereby avoiding the resource consumption associated with extensive repetitive testing. The application of machine learning in the field of civil engineering maintenance and diagnostics has started early and has yielded a substantial number of valuable research outcomes with practical engineering significance. However, in the domain of engineering structural design, the integration of intelligent technologies is still emerging. Existing research predominantly focuses on predicting material properties such as concrete strength, optimal mix ratios, erosion resistance, etc., while predictions concerning the performance of structural components are relatively scarce. Nevertheless, predicting component performance is fundamental to achieving intelligent structural design. Therefore, conducting predictive research on the performance and load-bearing capacity of structural components using machine learning methods holds significant importance.

Since John Lally, an American, first filled concrete in circular steel tubes as load-bearing column components and applied for a patent in 1897, steel tube concrete structures have been widely recognized and studied by the academic and engineering communities due to their advantages of high load-bearing capacity, good ductility, ease of construction, fire resistance, and cost-effectiveness. In steel tube concrete structures, rectangular steel tubes do not provide as significant confinement to the core concrete as circular steel tubes do. However, concrete-filled rectangular steel tube (CFRST) possesses the characteristics of strong plastic deformation capacity, good ductility, and excellent seismic performance, while also overcoming the design, construction, and usability inconveniences associated with the special cross-sectional shape of circular steel tube concrete structures. Additionally, concrete-filled rectangular steel tube structures have the advantages of high flexural stiffness and convenient node connections. Given the numerous advantages of CFRST columns, they have been widely applied in high-rise structures, subway stations, and other engineering projects. Therefore, research and application of CFRST columns hold significant value in the field of engineering. Axial compression is one of the typical loading conditions for steel tube concrete load-bearing members, and accurately predicting their bearing capacity is a crucial prerequisite for ensuring structural safety. Due to the influence of multiple factors, such as geometric parameters, material properties, and nonlinear interactions, the calculation of bearing capacity for concrete-filled rectangular steel tube is complex.

Researchers have conducted extensive experimental studies and theoretical analyses on the bearing capacity of CFRST columns, yielding fruitful results and establishing relevant design codes and technical regulations. These codes provide various theories and empirical formulas for the design of CFRST columns. The ultimate limit state theory used in EC 4 (1994) [1] and ACI 318-99 [2] considers CFRST columns equivalent to reinforced concrete columns, using simplified formulas to calculate the axial load-bearing capacity. The unified theory adopted in GJB 4142-2000 [3] and DBJ/T13-51-2020 [4] assumes the combined action of concrete and steel during the load-bearing process, no longer distinguishing between steel tubes and concrete. Instead, the overall geometric properties of the member (such as cross-sectional area and moment of inertia) and the composite performance indicators of steel tube concrete are used to calculate various load-bearing capacities of the member. The superposition theory ignores the interaction between the steel tube and concrete, treating the final bearing capacity under axial load as the sum of the concrete bearing capacity and the steel tube bearing capacity. Representative codes for this approach are AIJ (1997) [5] and DB/T29-57-2016 [6]. The pseudo-steel theory is based on steel structure design codes, where concrete is converted to steel using the elastic modulus, without changing the cross-sectional area of the steel tube. It considers the filled concrete as a means to increase the yield strength and elastic modulus of the steel tube, thereby calculating the relevant parameters of the equivalent steel tube and using the bearing capacity of the equivalent steel tube component as the bearing capacity of the prototype steel tube concrete component. The representative code for this theory is CECS 159:2004 [7].

Researchers have conducted extensive experimental studies and theoretical analyses on the bearing capacity of CFRST columns, achieving fruitful results and establishing relevant design codes and technical specifications. These codes encompass various theories and empirical formulas for the design of CFRST columns. However, there are significant differences in design codes and technical specifications among different countries, such as EC4 (1994), AISC-LRFD (1979) [8], and BS 5400 (1978) [9]. Even within the same country, such as China, the standards vary greatly, including CECS 159:2004, GJB 4142-2000, and DBJ/T13-51-2020, as shown in Table 1 for their corresponding applicability ranges. Each design code demonstrates different levels of accuracy and is only applicable to certain ranges of materials and geometric properties. Existing calculation models exhibit higher accuracy for CFRST columns using ordinary concrete strength and steel strength. However, using these models

to predict the bearing capacity of other types of CFRST columns, such as high-strength steel tube concrete and thin-walled steel tube concrete, can lead to significant errors. Nonetheless, with recent advancements in building materials, ultra-high-strength structural steel ranging from 690 MPa to 1300 MPa and ultra-high-strength concrete ranging from 120 MPa to 200 MPa have emerged for modern construction. The use of high-strength steel, high-strength concrete, and large-section profiles in steel tube concrete has become increasingly common to meet the requirements of heavy-duty design. The material strength and slenderness ratio often exceed the applicable range of the design codes. Therefore, developing a unified and efficient design method for CFRST columns is necessary and urgent, and the development of machine learning methods offers a new approach to address these issues. Machine learning methods make full use of the advantages of the big data era, leveraging the accumulated experimental data from different regions and periods over the past few decades. These methods directly explore the mapping relationship between the inputs (structural basic design parameters) and outputs (target performance indicators) in the data samples, thereby establishing accurate and stable prediction models. Compared to traditional "mechanics-driven" methods, this approach focuses on data, avoiding complex mechanical derivations and numerical implementations. It is a "data-driven" modeling method that can complement the "mechanics-driven" methods, leading to a more comprehensive and refined modeling method for predicting the axial compressive bearing capacity of CFRST columns.

Table 1 The applicability range of design codes for concrete-filled rectangular steel tube components.

code	EC 4 (1994)	AISC-LRFD (1979)	BS 5400 (1978)	CECS 159:2004	GJB 4142-2000	DBJ/T13-51-2020
Specimen type	**Cylinder**	**Cylinder**	**cube**	**cube**	**cube**	**cube**
$f_c^{'}orf_{cu}\left(Mpa\right)$	$21 \ll f_c^{'} \ll 70$	$20.7 \ll f_c^{'} \ll 55$	$f_c \gg 20$	$30 \ll f_{cu} \ll 80$	$30 \ll f_{cu} \ll 60$	$30 \ll f_{cu} \ll 90$
$f_y\left(Mpa\right)$	$235 \sim 355$	$\ll 379$	$275 \sim 355$	$235 \sim 420$	$235 \sim 390$	$235 \sim 420$
H/t	$52\sqrt{235/f_y}$	$\sqrt{3E_s/f_y}$	$\sqrt{3E_s/f_y}$	$60\sqrt{235/f_y}$	$40\sqrt{235/f_y}$	$60\sqrt{235/f_y}$

In recent years, preliminary research has emerged using machine learning methods to predict the axial compressive capacity of CFRST columns, and the relevant algorithms and database information are summarized in Table 2. It can be observed that the early studies had relatively small-scale databases. For example, the database established by Tien-Thinh Le et al. [10] consisted of only 102 specimens, and the column category was limited to short columns, which restricted the applicability range of the models developed. However, their research demonstrated that using neural networks to predict the load-bearing capacity of steel tube concrete exhibited high accuracy. Tran et al. and Du et al. developed databases with 300 and 302 specimens, respectively, and their proposed models further improved the generalization ability and applicability range, facilitating reliable and rapid prediction of the axial compressive capacity of rectangular CFST (Concrete-Filled Steel Tube) columns, suitable for practical design applications. However, the existing research still has the following limitations: 1) The size of the databases is relatively small (less than 400 specimens), representing only a small portion of the existing experimental data. A smaller database can lead to overfitting of the model, thereby reducing its predictive accuracy. 2) Most scholars have used a single machine learning method (such as ANN, SVM, DT), which exhibits poorer generalization ability compared to ensemble learning methods (such as RF, GDBT, XGBoost). Moreover, using only one machine learning method for load prediction lacks comparisons between different models. 3) Currently, there are only prediction models for the axial compressive capacity of short columns made of concrete-filled rectangular steel tube, while there is a lack of predictive research for long columns of the same material. 4) Different scholars have used different input parameters, and there has been a lack of exploration and analysis of dataset features, as well as the determination of feature correlation and feature selection methods. 5) The application of machine learning methods demonstrates the unique advantages of this approach in predicting the fundamental performance of concrete structures. However, most current research is based on "black box" models, which can provide accurate predictions based on input data but lack explanations for the model predictions. This limitation reduces the credibility and application scope of machine learning methods.

To this end, this study establishes a predictive model for the axial compressive capacity of CFRST columns based on machine learning methods. Based on a survey of 132 sets of tests conducted between 1962 and 2023, a database is established, including a total of 1,119 specimens, consisting of 460 short column specimens and 659 long column specimens of concrete-filled rectangular steel tube. A feature correlation heatmap is plotted to explore and analyze the dataset features, and the f_regression score function is used for feature selection to determine the input parameters of the machine learning model. Machine learning algorithms such as Lasso Regression, Artificial Neural Networks (ANN),

Random Forest (RF), and Extreme Gradient Boosting (XGBoost) are employed to predict the axial compressive capacity of concrete-filled rectangular steel tube. The predictive ability of the models for different load directions is studied, and suitable machine learning algorithms are selected through comparative analysis. Furthermore, a new feature parameter sensitivity analysis method based on SHAP (Shapley Additive Explanations) is used to interpret the machine learning prediction model and reflect the influence of each feature parameter on the final prediction value. The selected machine learning algorithms are compared and analyzed with the current load calculation methods in domestic and international codes and specifications to verify the accuracy of the established machine learning models. The aim is to provide reference for the intelligent prediction and design of the axial compressive capacity of steel tube concrete components.

Table 2 Summary of the machine learning predictive models for the axial compressive capacity of CFRST

Data Sources	Number of test pieces	B/mm	t/mm	L/mm	fy/Mpa	f'c/Mpa	Machine learning algorithm	Predictive parameter
Ref[10]	102	60-285	2.5-7.9	60-3600	192-395	25-85	ANN	N
Ref[11]	180	100-323	1.44-7.47	300-969	198-835	10.65-91.1	SVM	N
Ref[12]	314	60-324	2-11.70	295-3150	194.2-835	7.9-164.1	GPR	N
Ref[13]	392	77-323	1.90-12.50	330-3910	242-781	15-193	ANN	N
This research	1119	60-750	0.8-16	60-4135	176.7-1030.6	8-226	Lasso, ANN, RF, XGBoost	N

2 Establishment and Comparative Analysis of Machine Learning Models

2.1 The establishment of the database.

The dataset used in this study consists of 1,119 experimental data points, including 460 test data points for short CFRST columns and 659 test data points for long CFRST columns (short columns are defined as columns with $L/B \le 4$, and long columns are defined as columns with $L/B > 4$, where L is the length of the specimen and B is the length of the shorter side of the rectangular cross-section). These data points are collected from existing literature. Figure 1 presents a diagram of CFRST columns under axial loading together with their geometrical descriptions. Due to the wide range of data sources, the reported concrete strength in different studies is obtained from cylindrical, cubic, or prismatic specimens of different sizes, requiring strength conversion. The definition of unified compressive strength of concrete is of great significance for developing the experimental database and comparing steel tube concrete tests conducted worldwide. Considering that 86.5% of the specimens' concrete strength in the database is obtained from cylindrical specimens, according to the concrete structural design code, all specimens' concrete strength is converted to the strength of a standard cylindrical specimen with a diameter of 150mm and a height of 300mm (f'c) to achieve normalization of database parameters and reduce errors caused by the conversion process. See equations (1) and (2) for conversion formulas, and Table 3 lists the detailed conversion factors.

$$f_{ck} = 0.88 \times \alpha_1 \times \alpha_2 \times f_{cu,k} \tag{1}$$

$$f_c^{'} = \alpha_3 \times f_{cu,k} \tag{2}$$

Among them, f_{ck} is the standard value of the axial compressive strength of the concrete prism, $f_{cu,k}$ is the standard value of the axial compressive strength of the concrete cube, and $f_c^{'}$ is the standard value of the axial compressive strength of the concrete cylinder. $\alpha_1, \alpha_2, \alpha_3$ is the calculation coefficient, which is determined according to the concrete strength, see Table 3 for details.

There are 11 feature parameters, including the width of the steel tube section (B, short side), the height of the steel tube section (H, long side), the thickness of the steel tube wall (t), the length of the column (L), the slenderness ratio

(L/B), the aspect ratio of the section (H/B), the width-thickness ratio of the steel plate (H/t), the yield strength of the steel (fy), the compressive strength of the concrete cylinder (f'c), the elastic modulus of the concrete (Ec) and the elastic modulus of the steel (Es). Table 4 shows the statistical parameters of the 1119 test data points. From Table 4, it can be seen that the database covers a wide range of parameters. The range of section height H, aspect ratio H/B, and external depth-to-thickness ratio H/t of the specimens are 60 to 750 mm, 1 to 3.03, and 10.49 to 240, respectively. The range of specimen length L and slenderness ratio L/B are 60 to 4135 mm and 0.59 to 47.49, respectively. The yield strength fy ranges from 177.26 to 1030.6 MPa, and the compressive strength fc' of the concrete cylinders ranges from 8 to 173.85 MPa. Figure 2 presents the distribution of feature parameters for 1,119 experimental data.

Table 3 Detailed values of calculation coefficient $\alpha_1, \alpha_2, \alpha_3$

$f_{cu,k}$ / Mpa	α_1	α_2	α_3
≤ 40	0.76	1	0.79
50	0.76	0.9675	0.79
60	0.78	0.935	0.833
70	0.80	0.9025	0.857
80	0.82	0.87	0.875

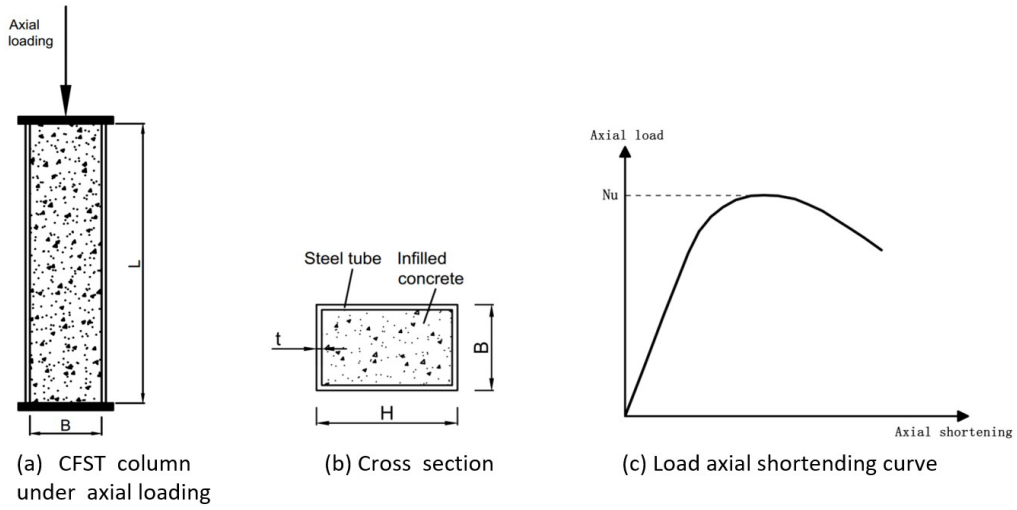

Figure 1. Diagram of CFRST column.

Table 4 Parameter statistics information

Feature parameter	Count	Mean	Std	Min	Max
B	1119	137.65	62.72	60	750
H	1119	155.67	70.05	60	750
t	1119	4.58	1.96	0.8	16
L	1119	1225.82	984.87	60	4135
L/B	1119	10.15	9.64	0.59	47.49
H/B	1119	1.16	0.30	1	3.03
H/t	1119	38.76	21.93	10.49	240
fy	1119	422.79	177.26	176.7	1030.6
f'c	1119	56.73	31.28	8	173.85
Ec	1119	37.68	6.20	23.4	52.52
Es	1119	200.11	3.03	182	226

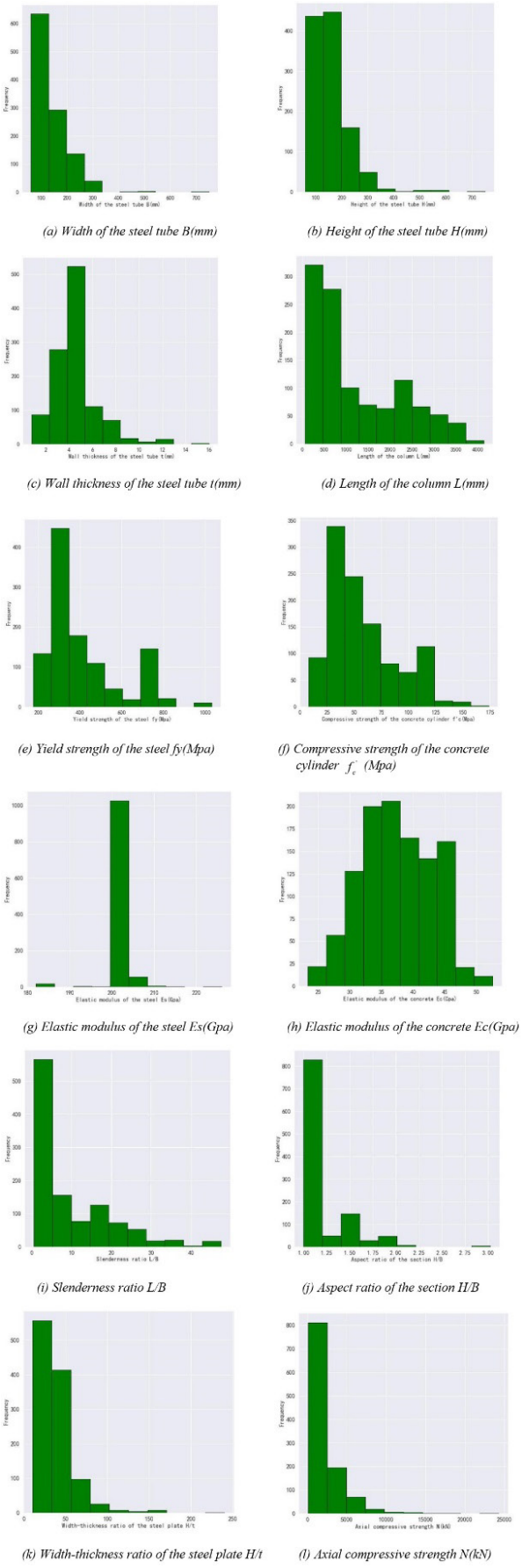

(a) Width of the steel tube B(mm)

(b) Height of the steel tube H(mm)

(c) Wall thickness of the steel tube t(mm)

(d) Length of the column L(mm)

(e) Yield strength of the steel fy(Mpa)

(f) Compressive strength of the concrete cylinder $f_c^{'}$ (Mpa)

(g) Elastic modulus of the steel Es(Gpa)

(h) Elastic modulus of the concrete Ec(Gpa)

(i) Slenderness ratio L/B

(j) Aspect ratio of the section H/B

(k) Width-thickness ratio of the steel plate H/t

(l) Axial compressive strength N(kN)

Figure 2 Statistical distribution of 1119 experimental data.

2.2 Data preprocessing and feature selection.

The axial compressive strength of rectangular concrete-filled steel tubes varies between 105.4 kN and 24294 kN, with an average value of 2235.31 kN. The probability density distribution of the axial compressive strength is shown in Figure 3a, indicating a noticeable left skewness. To improve the data handling capability of the model, this study applies the Box-Cox transformation to normalize the target values. The distribution of axial compressive strength of rectangular concrete-filled steel tubes before and after the transformation is shown in Figure 3.

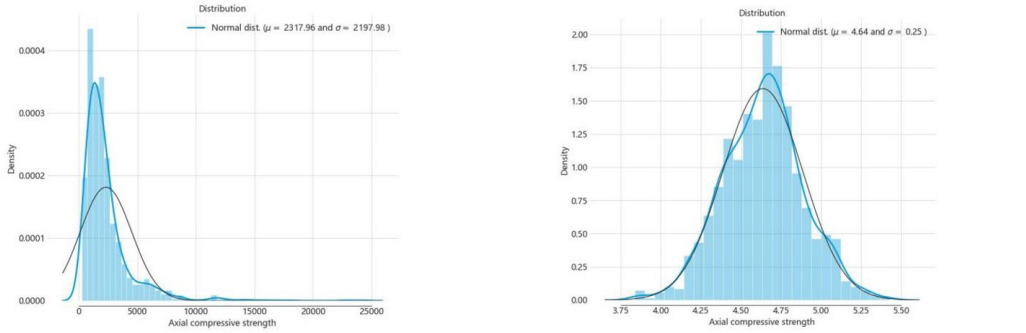

(a) axial compressive strength distribution chart

(b) After Box-Cox transformation, the axial compressive strength distribution chart

Figure 3 The axial compressive strength distribution chart

To explore and analyze the features of the dataset, a heatmap of feature correlation was generated. In the heatmap, lighter colors indicate higher correlation between two features, while darker colors indicate lower correlation. The heatmap of feature correlation with axial compressive strength is shown in Figure 4.

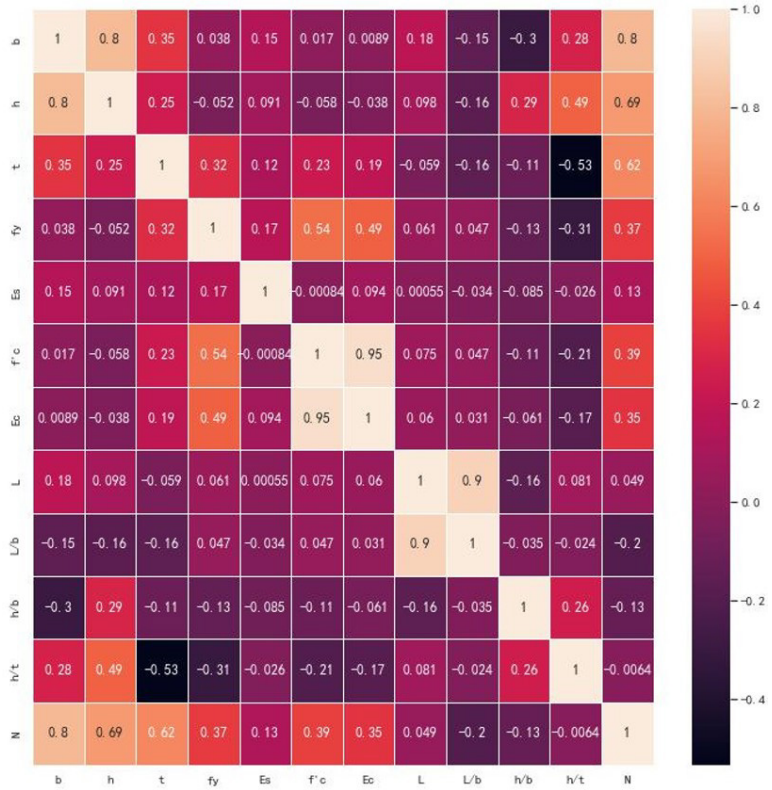

Figure 4 Partial variables and target variable (N) heatmap.

The axial compressive strength (N) is subjected to feature selection using the f_regression scoring function. F-Score was initially proposed by Chen from National Taiwan University and is a method to measure the discriminative power of features between two classes, distinct from the F1_score evaluation metric for classification problems. Based on this

method, effective feature selection can be achieved. A higher F-Score indicates a stronger discriminatory ability of the feature. The F-Score of all features is calculated for feature selection, and the F-Scores of the features are listed in Figure 5.

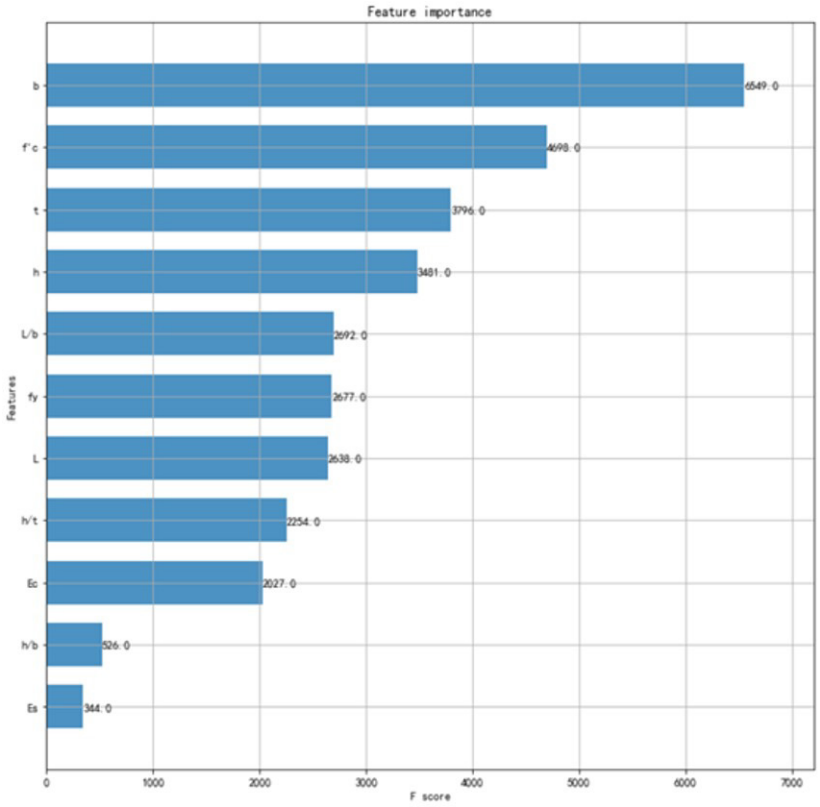

Figure 5. F_score of feature parameters.

Feature selection was performed based on the feature correlation heatmap and the calculation of F-Score importance values. Among the geometric parameters of the rectangular steel tube-concrete columns, the parameters D, B, and t showed strong positive correlations with N (axial compressive strength), while the aspect ratio (L/B) and the aspect ratio of the section (H/B) exhibited strong negative correlations with N. Regarding the material parameters of the rectangular steel tube-concrete columns, the parameters fy, f'c, and Ec demonstrated strong positive correlations with N. However, the elastic modulus of the steel material showed a weak positive correlation with N, with a correlation coefficient of only 0.13. Furthermore, its F-Score value was the lowest at 344.0, indicating that it had a minimal contribution to N. Considering that the distribution of the elastic modulus values in the database ranged from 182 to 226, with 75% of the values being 200 GPa and having low fluctuation, this feature parameter was removed. Although the width-to-thickness ratio of the steel plate (H/t) exhibited a weak negative correlation with N, with a correlation coefficient of only -0.0064, its F-Score value was relatively high at 2254.0. Previous studies have shown that the width-to-thickness ratio of the plate (H/t) is an important parameter affecting the local buckling of the steel tube wall, which in turn reduces the load-carrying capacity and ductility of the structure. Therefore, this feature parameter was retained. After feature selection and processing, the resulting dataset consisted of 1119 samples. Taking into account the influences of different parameters on the load-bearing capacity of the steel tube-concrete columns, 10 input parameters (B, H, t, L, L/B, H/B, H/t, fy, f'c, Ec) were selected for predicting the axial compressive strength of rectangular steel tube-concrete columns. Once the database collection was completed, the 1119 experimental data points were randomly divided into training and testing datasets in approximately a 7:3 ratio, with 783 samples assigned to the training dataset and the remaining 336 samples assigned to the testing dataset.

2.3 Algorithm evaluation metrics

In this paper, the coefficient of determination (R^2), mean absolute error (MAE), and root mean square error (RMSE) are selected as the evaluation metrics to measure the model performance. The calculation formulas are shown in Equation (3) to Equation (5).

$$R^2\left(y_i,\widehat{y_i}\right)=1-\frac{\sum_{i=1}^{n}\left(y_i-\widehat{y_i}\right)^2}{\sum_{i=1}^{n}\left(y_i-\overline{y_i}\right)^2} \tag{3}$$

$$MAE\left(y_i,\widehat{y_i}\right)=\frac{1}{n}\sum_{i=1}^{n}\left|y_i-\widehat{y_i}\right| \tag{4}$$

$$RMSE\left(y,\widehat{y_i}\right)=\sqrt{\frac{1}{n}\sum_{i=1}^{n}\left(y_i-\widehat{y_i}\right)^2} \tag{5}$$

Where y_i represents the actual values of the samples, $\widehat{y_i}$ represents the predicted values, and n represents the number of samples.

The coefficient of determination reflects the proportion of the total variation of the dependent variable that can be explained by the regression relationship with the independent variables. It represents the degree of fit of the regression results to the observed values. The coefficient R^2 takes values between 0 and 1, where a larger coefficient of determination indicates a better model performance. The Mean Absolute Error (MAE) is the average of the absolute differences between the predicted values and the actual values. The Root Mean Square Error (RMSE) is a measure that reflects the extent of differences between the predicted values and the actual values. Both MAE and RMSE have the same units of measurement, but RMSE first squares the errors, then sums them, and takes the square root, amplifying the differences between larger errors. Compared to MAE, RMSE tends to have larger values and more directly reflects the true errors. Smaller values of MAE and RMSE indicate more accurate model predictions.

2.4 Training and comparative experiments of machine learning models.

Machine learning methods can be divided into linear regression algorithms, single learning methods, and ensemble learning methods. In this study, we employed one linear regression algorithm (Lasso), one single learning method (ANN), and two ensemble learning methods (RF, XGboost), totaling four algorithms, to predict and compare the axial compressive strength of CFRST columns. The features and labels from the dataset were inputted into the models, and the data were divided into training and testing sets. Machine learning algorithm models were trained on the training set and used to make predictions on the testing set. Grid search and 10-fold cross-validation methods were employed to determine the optimal hyperparameters for hyperparameter tuning.

Figure 6 shows the comparison between the predicted values and the actual values for the four models. It can be visually observed that compared to Lasso Regression and ANN, the predicted values of axial compressive strength based on RF and XGBoost are more concentrated within the error limit of ±15%. This indicates that the prediction models for axial compressive strength of concrete-filled rectangular steel tube based on RF and XGBoost algorithms have better predictive performance on the samples.

Table 5 presents the test results of the four machine learning prediction models. According to the results, the Extreme Gradient Boosting (XGBoost) model achieves the best performance in terms of MAE, RMSE, MSE, and R^2. It demonstrates strong generalization ability and high prediction accuracy. Random Forest (RF) and Artificial Neural Network (ANN) also exhibit reasonable accuracy. However, the Lasso Regression model shows poor predictive accuracy, with a test set coefficient of determination of only 0.865 and a MAE of 520.31. Therefore, the following section will employ the XGBoost model for feature analysis and prediction of the ultimate torsional strength.

Table 5 Evaluation metrics of different machine learning prediction models.

predictive model	Number set	R^2	RMSE	MAE
Lasso	Train	0.862	884.73	591.28
	Test	0.865	725.34	520.31
ANN	Train	0.912	707.14	444.48
	Test	0.916	573.52	385.25
RF	Train	0.988	260.83	102.95
	Test	0.954	425.78	235.50
XGBoost	Train	0.998	57.61	16.26
	Test	0.980	294.82	148.63

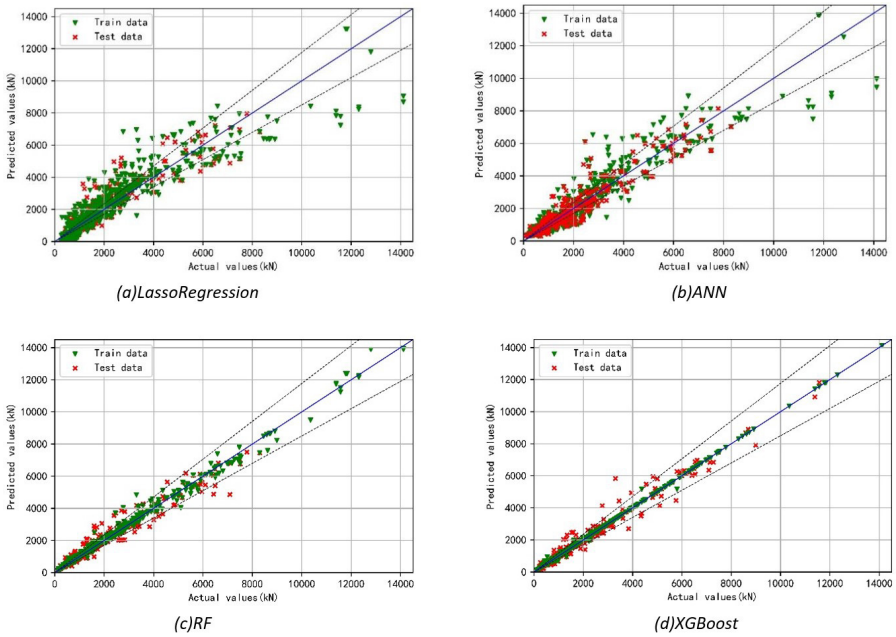

Figure 6 The prediction performance of LassoRegression, ANN, RF, and XGBoost machine learning models.

3. Feature importance analysis based on the SHAP method

The application of machine learning methods has demonstrated their unique advantages in predicting the basic performance of steel-concrete structures. However, most of the current research focuses on “black box” models, which can provide accurate predictions based on inputs but lack interpretability. This limitation reduces the credibility and applicability of machine learning methods. Traditional methods like Feature Importance can intuitively reflect the importance of features but cannot determine the relationship between features and the final prediction. SHAP (SHapley Additive exPlanations) uses a feature attribution method to calculate the attribution values of features, which can reflect the impact of each feature on the final prediction and indicate the positive or negative influence, thus enhancing the interpretability of the model. SHAP provides powerful data visualization capabilities to display the model and explanation results, making it widely applicable for interpreting complex algorithm models. Therefore, using the SHAP algorithm to explain the XGBoost model allows us to analyze the impact of each feature on the predicted value and identify the key parameters in estimating axial load-bearing capacity.

3.1 The global interpretation of the experimental database

The SHAP method can be used to explore the influence of input variables on the final axial compressive load capacity prediction of XGBoost model for rectangular steel-concrete columns. The important factors of the input variables are shown in Figure 7a. The higher the SHAP value, the greater the variable's influence. The main influences of the input variables on the axial compressive load capacity of rectangular steel-concrete columns, ranked by importance, are B, t, fy, f'c, H, L/B, and Ec. It is important to note that the Shapley values are based on average prediction results. It can be observed that B is the most important feature, which increases the predicted axial compressive load capacity by an average of 926.48 kN (shown as 926.48 on the x-axis). The importance of t relative to B is approximately 73%. The contributions of L, H/t, and H/B are smaller compared to the seven major features, with their importance being approximately 6.6%, 2.7%, and 1.6% of B, respectively.

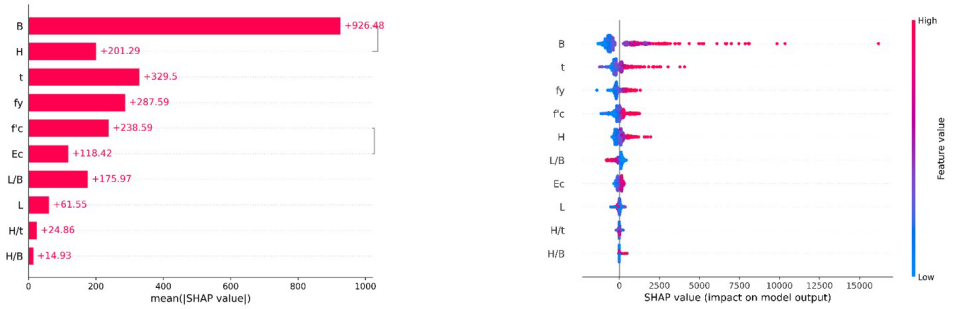

(a) Global feature importance analysis. *(b) SHAP feature distribution summary plot.*

Figure 7 Global interpretation using SHAP method.

Figure 7b displays the distribution of SHAP values for each feature parameter and illustrates the corresponding impact trends. In the figure, the horizontal axis represents specific SHAP values, and the vertical axis represents input variables (i.e., feature parameters) sorted by their importance. Each point represents an individual sample from the entire dataset, colored from low (blue) to high (red) according to the corresponding feature's value. Positive or negative SHAP values indicate positive or negative correlations between the feature and the output parameter (i.e., N). Therefore, Figure 7b not only demonstrates which features are important but also reveals how each feature parameter influences the axial compressive load capacity (N). The section width B and wall thickness t are the most critical variables, with larger values of B and t resulting in larger SHAP values and greater contributions to the axial compressive load capacity. Similarly, larger values of the steel yield strength fy, concrete compressive strength f'c, and section height H will increase the corresponding SHAP values, leading to higher axial compressive load capacity. On the other hand, for feature parameters such as aspect ratio L/B, section height-to-width ratio H/B, and plate width-to-thickness ratio H/t, there is a decreasing trend in axial compressive load capacity as these values increase. In contrast, the aspect ratio L/B has a significant negative impact on most samples. The tail typically extends to the left rather than the right, indicating that extreme L/B values significantly reduce the axial compressive load capacity.

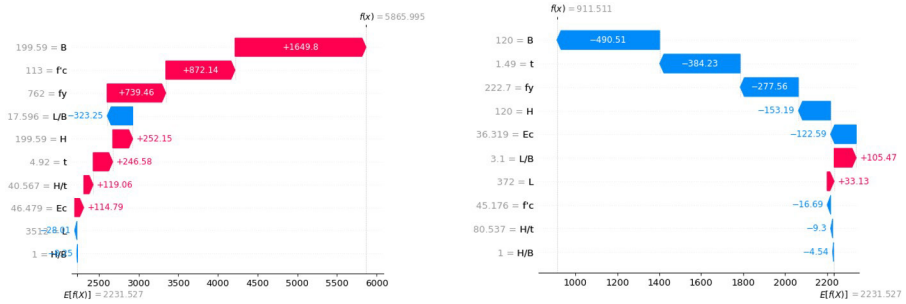

(a) Sample 1: CB40-SL3(B) *(b) Sample 2: 4-4P*

Figure 8 The individual model interpretation results of the SHAP method.

3.2 The local interpretation of the experimental database

In addition to providing global explanations for the database, SHAP values also provide local explanations for each individual sample. Two representative samples, a long column and a short column (CB40-SL3(B)[14] and 4-4P[15]), are selected for illustration as shown in Figure 8. The SHAP method decomposes the predicted axial compressive capacity of CFST columns into the sum of the influences from each feature parameter. The average predicted torsional resistance is 2231.527 kN, serving as the baseline value. Each feature parameter that contributes to higher or lower predictions (compared to the baseline) is displayed in red or blue, respectively. As shown in Figure 8a, for sample 1, B is the most critical feature parameter with a positive influence on the axial compressive capacity, having a SHAP value of 1649.8 kN. Similarly, f'c, fy, and H have positive influences on the shear capacity, with SHAP values of 872.14 kN, 739.46 kN, and 252.15 kN, respectively. L/B and L are the most critical feature parameters with negative effects on the axial compressive capacity, having SHAP values of -323.25 kN and -28.01 kN, respectively. By combining the baseline values and SHAP values for all feature parameters, the final predicted shear capacity is 5865.995 kN, which is close to the experimental value of 5896 kN. For sample 2, as shown in Figure 8b, L/B and L are typical positive feature parameters with SHAP values of 105.47 kN and 33.13 kN, respectively. B, t, fy, and H are typical negative feature parameters with SHAP values of -490.51 kN, -384.23 kN, -277.56 kN, and -153.19 kN, respectively. The final predicted shear capacity is 911.511 kN, which is close to the experimental value of 916 kN.

3.3 Feature dependency of the prediction results

SHAP can also reveal the feature dependency of the prediction results, that is, how the SHAP values change with the variation of input variables. This complements the SHAP feature distribution summary plot and provides more detailed insights into how SHAP values vary with feature values. Figure 9 presents the results for each feature parameter. It can be observed that the SHAP values of B, t, fy, f'c, and Ec increase with the values of the corresponding feature parameters, while the SHAP values of L and L/B decrease with increasing feature parameter values. This indicates a positive correlation between B, t, fy, f'c, Ec, and the axial compressive strength of the rectangular steel-reinforced concrete column, while L and L/B show a negative correlation. From Figure 9j, it can be seen that H/t exhibits an increasing trend in SHAP values with increasing feature parameter values up to 30, indicating an increase in the compressive strength. However, for H/t values above 30, the SHAP values decrease with increasing feature parameter values, indicating a decrease in the compressive strength. Furthermore, from Figure 9i, it is evident that H/B shows a slow increase in compressive strength with increasing feature parameter values below 1.5, while above 1.5, H/B exhibits a gradual decrease in compressive strength with increasing feature parameter values.

SHAP can also reveal the interaction effects among different feature parameters. Figure 10 presents the interaction results for six key feature parameters. Figure 10a shows the interaction between the section width B and the section height H. When the section height H is within the range of 0 to 125mm, the SHAP value of B slowly increases with increasing parameter values. However, when H is greater than 125mm, the SHAP value of B rapidly increases with increasing parameter values. From Figures 10b, c, e, and f, it can be observed that regardless of the size of fy and f'c, the SHAP values of B and t increase with increasing parameter values. Figure 10d displays the interaction between the section height H and the wall thickness t. When H is less than 120mm, regardless of whether t is large or small, the SHAP value of H is negative and negatively correlated with the axial compressive strength. However, when H is greater than 120mm, the SHAP value of H becomes positive and positively correlated with the axial compressive strength. When H is between 120mm and 320mm, the SHAP value of H rapidly increases with increasing parameter values. When H is greater than 320mm, the SHAP value of H increases slowly. From Figures 10g, h, and i, it can be observed that regardless of the size of t, fy, and f'c, when the aspect ratio L/B is less than 6, the SHAP value of H is positive and positively correlated with the axial compressive strength. However, when the aspect ratio L/B is greater than 6, the SHAP value of H is negative, and it decreases with increasing parameter values, showing a negative correlation with the axial compressive strength.

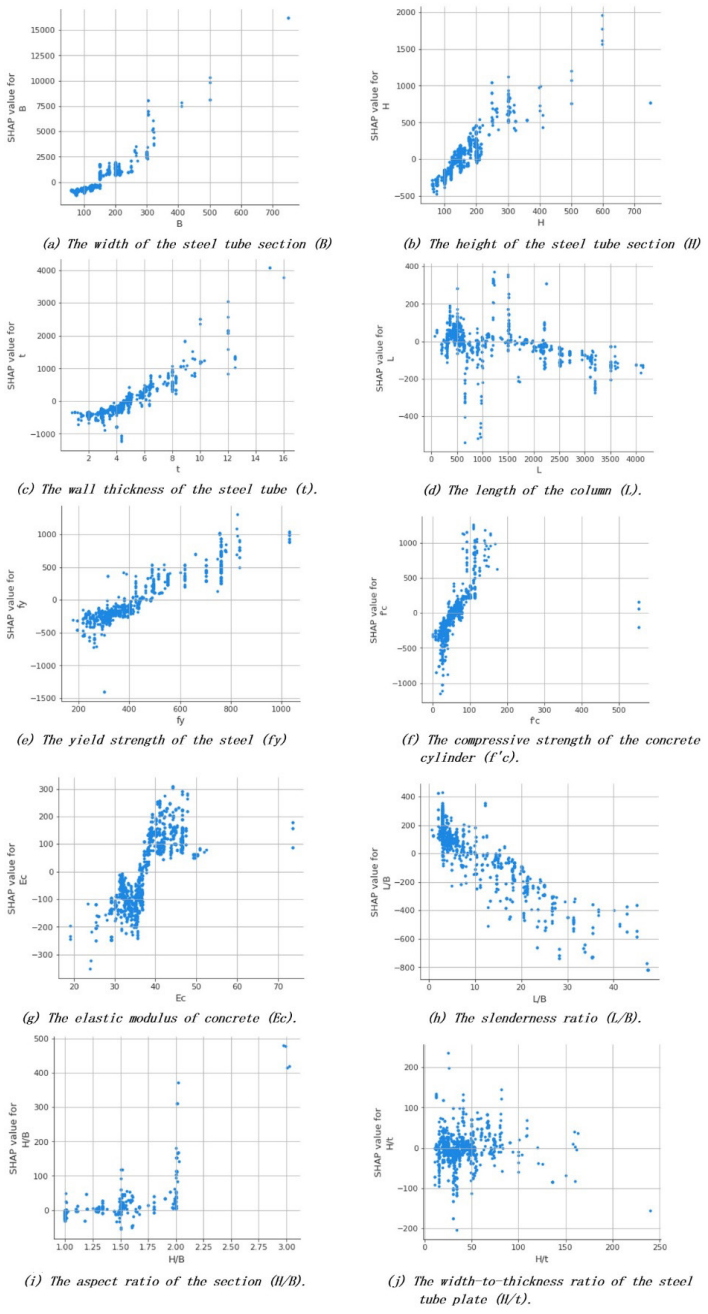

(a) The width of the steel tube section (B)

(b) The height of the steel tube section (H)

(c) The wall thickness of the steel tube (t).

(d) The length of the column (L).

(e) The yield strength of the steel (fy)

(f) The compressive strength of the concrete cylinder (f'c).

(g) The elastic modulus of concrete (Ec).

(h) The slenderness ratio (L/B).

(i) The aspect ratio of the section (H/B).

(j) The width-to-thickness ratio of the steel tube plate (H/t).

Figure 9 The impact patterns of each feature parameter on axial compressive capacity.

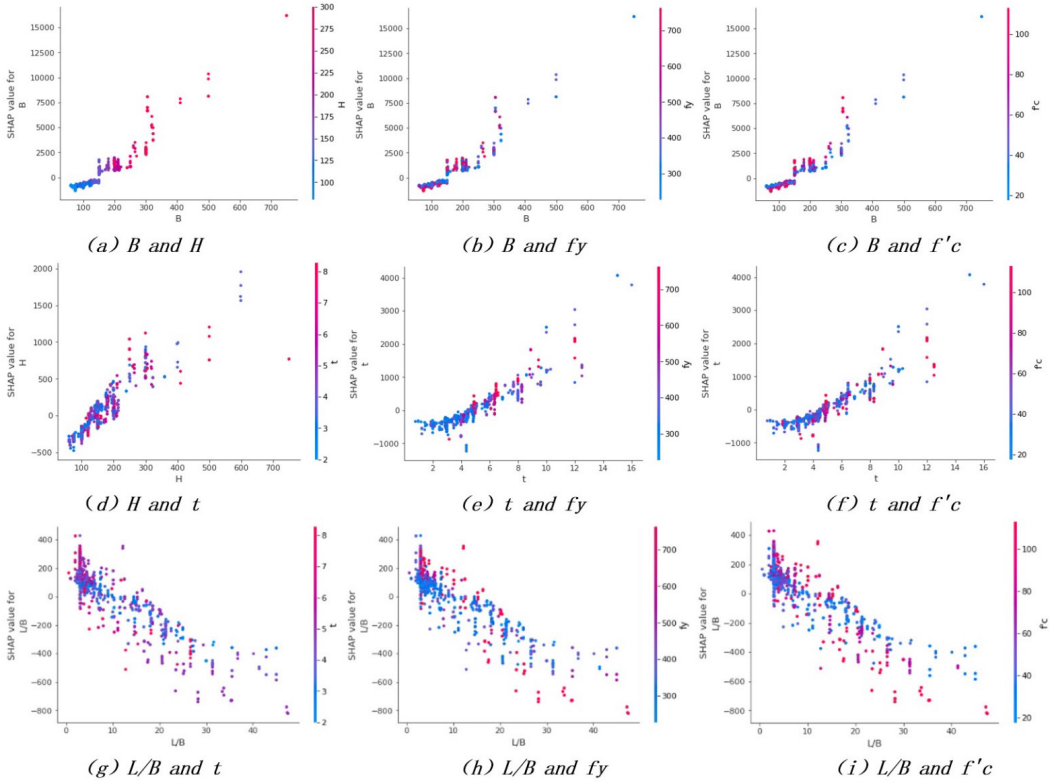

Figure 10 The interaction relationships among different feature parameters.

4. Comparison between XGBoost prediction model and existing standards.

Many design codes for steel and composite materials provide calculation methods and empirical formulas for the axial load-carrying capacity of CFRST columns. These include European standard EC4 (1994), American standard AISC-LRFD (1979), British standard BS 5400 (1978), as well as domestic standards such as CECS 159:2004, GJB 4142-2000, and DBJ/T13-51-2020. The empirical calculation formulas of each standard are listed in Table 6. Previous studies have often focused only on predicting the axial load-carrying capacity of short columns, while in practical engineering, columns are often long. The predictive performance of the XGBoost machine learning model for short and long columns is compared and analyzed against the load calculation methods of these six existing standards, both domestic and international, to validate the accuracy of the XGBoost model.

Table 6 The empirical design formulas in each standard.

Code	category	empirical design formula
EC4(1994)	short column	$N_{us} = \frac{f_y}{\gamma_s} \bullet A_s + \frac{f_c'}{\gamma_c} \bullet A_c$
	long column	$N_{ul} = \chi \bullet \left(\frac{f_y}{\gamma_s} \bullet A_s + \frac{f_c'}{\gamma_c} \bullet A_c \right)$
CECS:159:2004	short column	$N_{us} = f_y \bullet A_s + f_{ck} \bullet A_c$
	long column	$N_{ul} = \varphi \bullet \left(f_y \bullet A_s + f_{ck} \bullet A_c \right)$
GJB 4142-2000	short column	$N_{us} = A_{sc} \bullet \left(1.212 + \alpha \bullet \xi_o + \beta \bullet \xi_o^2 \right) \bullet f_c$
	long column	$N_{ul} = \Phi A_{sc} \bullet \left(1.212 + \alpha \bullet \xi_o + \beta \bullet \xi_o^2 \right) \bullet f_c$
AISC-LFRD(1999)	short column long column	$N_u = \begin{cases} \left(0.658^{\lambda^2} \right) F_{my} A_s \ldots\ldots\ldots\ldots (\lambda_c \le 1.5) \\ \left(0.887 / \lambda_c^2 \right) F_{my} A_s \ldots\ldots\ldots\ldots (\lambda_c \succ 1.5) \end{cases}$
BS 5400(1978)	short column	$N_{us} = 0.85 k_1 \bullet \left(0.91 A_s f_y + 0.45 A_c f_{cu} \right)$
	long column	$N_{ul} = k_2 \bullet \left(0.91 A_s f_y + 0.45 A_c f_{cu} \right)$
DBJ/T13-51-2020	short column	$N_{us} = A_{sc} \bullet \left(1.18 + 0.85 \theta_{sc} \right) \bullet f_c$
	long column	$N_{ul} = \varphi A_{sc} \bullet \left(1.18 + 0.85 \theta_{sc} \right) \bullet f_c$

Table 7 Evaluation metrics for the prediction capability of the XGBoost model and existing standards.

predictive model	Number set	R^2	RMSE	MAE
EC4(1994)	short column	0.919	848.03	626.20
	long column	0.836	563.85	427.36
CECS 159:2004	short column	0.951	660.67	434.74
	long column	0.858	524.77	377.39
GJB 4142-2000	short column	0.806	1315.11	859.75
	long column	0.709	751.75	501.48
AISC-LFRD(1979)	short column	0.966	546.61	370.22
	long column	0.899	463.59	312.40
BS 5400(1978)	short column	0.892	981.11	698.62
	long column	0.761	681.35	511.97
DBJ/T13-51-2020	short column	0.917	858.74	628.63
	long column	0.808	611.31	458.52
XGBoost	short column	0.973	371.81	173.77
	long column	0.969	233.22	172.28

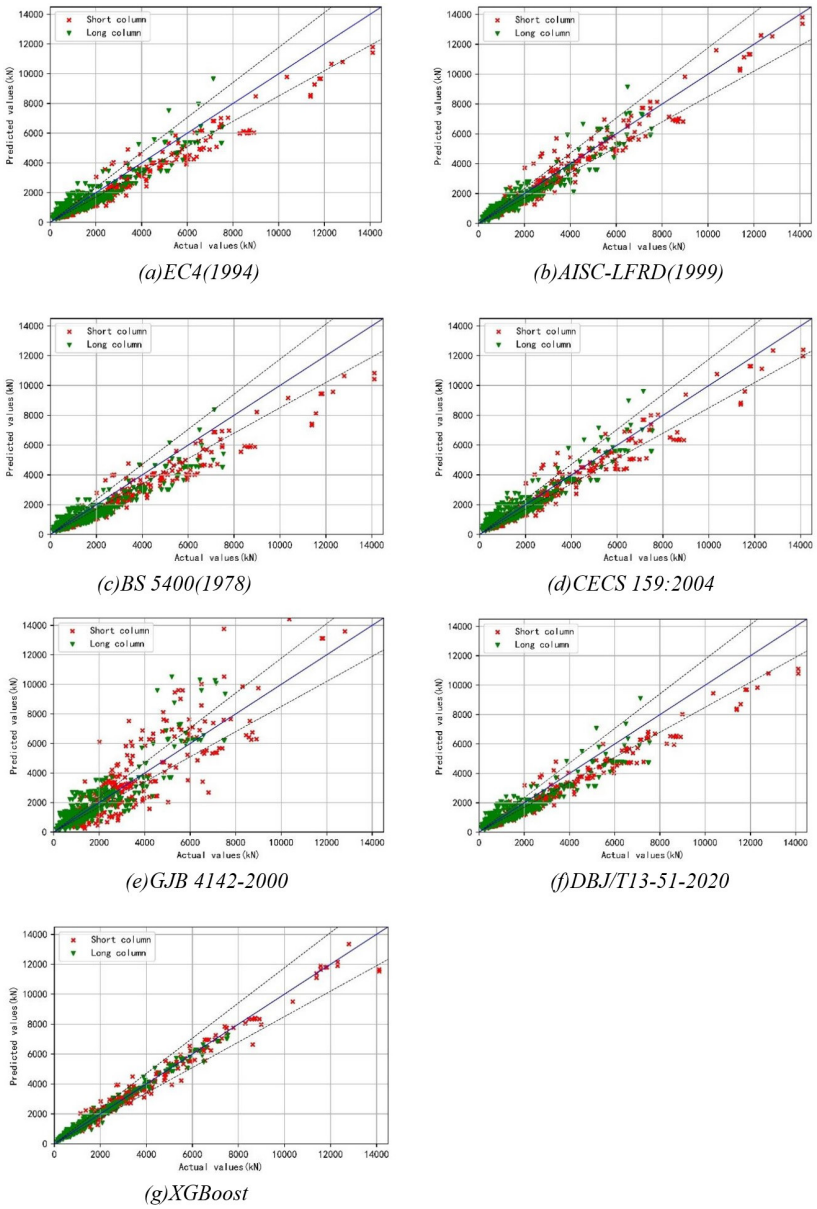

Figure 11. Prediction performance of the XGBoost model and six existing standards.

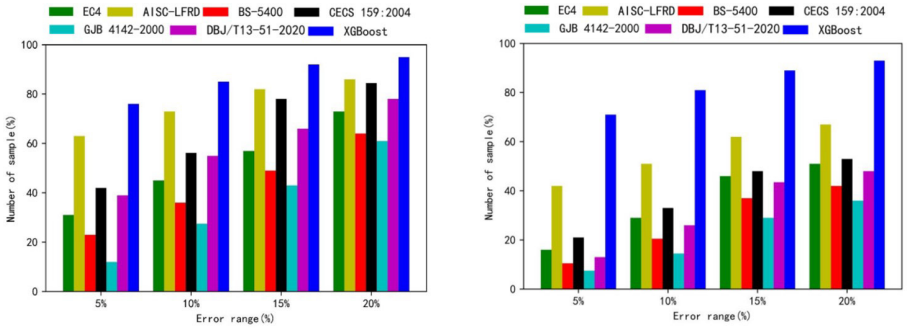

(a) short column data (b) long column data

Figure 12. Distribution of error range

Table 8. Error range of short column data prediction.

Error range(%)	The number of data within the error range and the corresponding percentage						
	EC4	AISC-LFRD	BS-5400	CECS159:2004	GJB4142-2000	DBJ/T13-51-2020	XGBoost
±5%	143	290	106	193	55	179	350
	(31%)	(63%)	(23%)	(42%)	(12%)	(39%)	(76%)
±10%	207	336	166	259	127	253	391
	(45%)	(73%)	(36%)	(56.2%)	(27.5%)	(55%)	(85%)
±15%	262	377	225	359	198	304	423
	(57%)	(82%)	(49%)	(78%)	(43%)	(66%)	(92%)
±20%	336	396	295	389	281	359	437
	(73%)	(86%)	(64%)	(84.5%)	(61%)	(78%)	(95%)

Table 9. Error range of long column data prediction.

Error range(%)	The number of data within the error range and the corresponding percentage						
	EC4	AISC-LFRD	BS-5400	CECS159:2004	GJB4142-2000	DBJ/T13-51-2020	XGBoost
±5%	105	277	69	138	49	86	468
	(16%)	(42%)	(10.5%)	(21%)	(7.5%)	(13%)	(71%)
±10%	191	336	135	217	96	171	534
	(29%)	(51%)	(20.5%)	(33%)	(14.5%)	(26%)	(81%)
±15%	303	409	244	316	191	287	587
	(46%)	(62%)	(37%)	(48%)	(29%)	(43.5%)	(89%)
±20%	336	442	277	349	237	316	613
	(51%)	(67%)	(42%)	(53%)	(36%)	(48%)	(93%)

Figure 11 shows the comparison between the predicted values and actual values of the XGBoost model and six existing specifications. Table 7 presents the testing results of the predictive model. For short columns, the XGBoost-based predictive model has achieved some improvement compared to existing models. Compared to EC4, BS 5400, CECS 159:2004, GJB 4142-2000, and DBJ/T13-51-2020, the predicted axial compressive capacity values of AISC-LRFD and XGBoost are more concentrated within a ±15% error limit, with determination coefficients of 0.966 and 0.973, mean absolute errors (MAE) of 370.22 and 173.77, and root mean square errors (RMSE) of 546.61 and 371.81, respectively. For long columns, the accuracy of the XGBoost-based predictive model is significantly higher than the existing models, with a determination coefficient of 0.969 and MAE and RMSE values of 172.28 and 233.22, respectively.

The error distributions of all models are also plotted in Figure 12, and the summary of data for short columns and long columns is provided in Tables 8 and 9, respectively. It can be observed that the proposed XGBoost-based predictive model demonstrates superior accuracy for long column predictions compared to existing models, especially within a small error range. For short column predictions, it also shows some improvement compared to existing models within a small error range. However, for larger error ranges, the XGBoost-based model only provides slight improvements compared to existing models. For instance, within a 5% error range, the proposed GBT model achieves an accuracy rate of 93% for long column predictions, which is nearly twice that of existing models. Among the six considered design specifications, AISC-LRFD offers the best predictions for short columns, with a determination coefficient of 0.966, MAE

and RMSE values of 370.22 and 546.61, and a prediction accuracy rate of 63% within a 5% error range. These values surpass CECS 159:2004 with 0.951, 434.74, 660.67, and 42%, respectively, but are much better than GJB 4142-2000 with 0.806, 859.75, 1315.11, and 12%. For long columns, AISC-LRFD also provides the best predictions, with a determination coefficient of 0.899, MAE and RMSE values of 312.40 and 463.59, and a prediction accuracy rate of 42% within a 5% error range. These values outperform CECS 159:2004 with 0.858, 377.39, 524.77, and 21%, respectively, but are significantly better than GJB 4142-2000 with 0.709, 501.48, 751.75, and 7.5%.

Therefore, it can be concluded that the proposed XGBoost-based model not only exhibits the best performance in predicting the strength of CFRST columns for both short and long columns, but also demonstrates superior generalization capability and accuracy.

5 CONCLUSION

1. Reasonable data preprocessing methods and correlation analysis are applied to determine the input parameters of the machine learning model in a scientifically and logically manner, considering the different correlations between geometric and material parameters and the bearing capacity of rectangular steel tube-concrete columns.
2. Ensemble learning methods (RF, XGBoost) outperform linear regression algorithm (Lasso) and single learning method (ANN) in predicting the axial compressive strength of rectangular steel tube-concrete columns. Among them, the XGBoost machine learning model exhibits the best performance, demonstrating superior generalization ability and highest prediction accuracy.
3. Based on the XGBoost prediction model, feature importance analysis using the SHAP method is conducted to identify the main factors influencing the axial compressive strength of rectangular steel tube-concrete columns. These factors, ranked from strongest to weakest, are B, t, fy, f'c, H, L/B, and Ec. Local interpretations are provided for selected samples, which demonstrate high accuracy in predicting their outcomes. The analysis also reveals the feature dependencies and interaction effects among the feature parameters of CFRST columns' axial compressive strength.
4. The predictive performance of the XGBoost machine learning model is compared with the bearing capacity calculation methods of six existing standards, both domestically and internationally. The XGBoost model exhibits significantly higher accuracy in predicting the bearing capacity of long columns compared to the current standards. Moreover, its accuracy in predicting short columns is further improved. Among the six considered standards, AISC-LRFD demonstrates the best prediction accuracy for both short and long columns.

Author's Contributions: Conceptualization, Tuo Lei and Jianxiang Xu; Methodology, Jianxiang Xu and Shuangfei Liang; Investigation, Zhimin Wu and Shuangfei Liang; Writing - original draft, Tuo Lei and Jianxiang Xu; Software, Zhimin Wu and Shuangfei Liang; data curation, Shuangfei Liang and Zhimin Wu; Validation, Jianxiang Xu and Shuangfei Liang; Writing – review & editing, Jianxiang Xu and Tuo Lei; Supervision, Tuo Lei.

Editor: Marcílio Alves

References

[1] Euro Code 4.Design of composite steel and concrete structures,Part,1: General Rules and rules for buildings(together with United Kingdom National Application Document(S). DDENV 1994—l;1994, British Standards Institution, London WIA2BS, 1994.

[2] ACI 318-99, Building code requirements for structural concrete and commentary S . Farmingtion Hills(Ml), American Concrete Insttute. Detroit, USA, 1999.

[3] GJB 4142-2000, Technical regulations for early-strength composite structures for emergency repair of military ports in wartime [S].117[s].

[4] Fujian Province Engineering Construction Standard DBJ/T13-51-2020 Technical Specification for Steel Tube Concrete Structures [s] (in Chinese).

[5] AIJ, Recommendations for design and construction of concrete filled steel tubular structures[S], Architectural Institute of Japan(AIJ) Tokyo, Japan, 1997.

[6] Tianjin Engineering Construction Standard DB/T29-57-2016 Tianjin Steel Structure Residential Design Regulations [S] (in Chinese.

[7] China Engineering Construction Standardization Association Standard CECS 159:2004 Technical Specification for Concrete-filled rectangular steel tube Structure [S] Beijing . (in Chinese).

[8] AISC-LRFD,Load and resistance factor design specification for structural steel buildings,2nd[S], American Institute of Steel Conrstruction(AISC) Chicago, USA,1979.

[9] British Standards Institutions, BS 5400 Steel,concrete and composite bridges,parts:Code of practice for design of composite bridges[s] London,UK, 1978.

[10] Le, T. T., Asteris, P. G., & Lemonis, M. E. (2021). Prediction of axial load capacity of rectangular concrete-filled steel tube columns using machine learning techniques. Engineering with Computers, 1-34.

[11] Ren, Q., Li, M., Zhang, M., Shen, Y., & Si, W. (2019). Prediction of ultimate axial capacity of square concrete-filled steel tubular short columns using a hybrid intelligent algorithm. Applied Sciences, 9(14), 2802.

[12] Le, T. T. (2022). Practical machine learning-based prediction model for axial capacity of square CFST columns. Mechanics of Advanced Materials and Structures, 29(12), 1782-1797.

[13] Tran, V. L., Thai, D. K., & Kim, S. E. (2019). Application of ANN in predicting ACC of SCFST column. Composite Structures, 228, 111332.

[14] Goode, C. D., & Lam, D. (2011). Concrete-filled steel tube columns-tests compared with Eurocode 4. In Composite Construction in Steel and Concrete VI (pp. 317-325).

[15] DENAVIT M. Steel-concrete composite column database [DB / OL]. [2021-10-5]. http://mark.denavit.me/Composite-Column-Database/.